

UV-Curable Powder Coatings Based on Dendritic Poly(ether-amide)

Huanyu Wei, Hongbo Liang, Jianhua Zou, Wenfang Shi

Department of Polymer Science and Engineering, University of Science and Technology of China, Hefei, Anhui, 230026, P. R. China

Received 30 April 2002; accepted 25 November 2002

ABSTRACT: Semi-crystalline dendritic poly(ether-amide)s were synthesized by modifying hydroxyl end-groups of dendritic poly(ether-amide) with aromatic urethane acrylate and octadecyl isocyanate. The ratio of these modifiers can adjust the final properties of products to fulfill the requirements of UV-curable powder coatings. These UV-curable semi-crystalline dendritic poly(ether-amide)s have a T_g in the range of 41–45°C and a T_m of around 120°C. Their thermal behavior and semi-crystalline properties were studied by DSC and XRD. The photopolymerization kinetics was

investigated by Photo-DSC. The residual unsaturation, thermal stability, and hardness of the UV-cured films were also studied. The obtained results show that these semi-crystalline dendritic poly(ether-amide)s may be used as prepolymers in UV-curable powder coating systems. © 2003 Wiley Periodicals, Inc. *J Appl Polym Sci* 90: 287–291, 2003

Key words: powder coating; UV curing; dendritic poly(ether-amide); semi-crystalline

INTRODUCTION

Powder coatings have many advantages compared with traditional liquid coatings. One of the main advantages is that they are zero-volatile organic compounds (VOC) and nontoxic systems without the addition of solvents for thermally curing systems or multifunctional monomers for UV curing systems. UV-curable powder coating systems are the combination of powder coatings with UV curing technology. When applied to heat-sensitive materials such as wood, plastic, medium density fiberboard, and pre-assembled articles, such as motors and gearboxes, UV-curable powder coatings are preferred since they offer the possibility of cure at temperatures as low as 100–120°C and a complete cure cycle in 40–150 s compared with 15–30 min at 180–200°C for conventional thermal-curable powder coatings.^{1,2}

For a UV-curable powder coating the most important requirements are high stability at room temperature and high reactivity when exposed to UV irradiation. To ensure the stability during handling, transportation, and storage, the powder should have a high glass transition temperature (T_g). On the other hand, to form a completely homogeneous and even film at a lower temperature before curing, it is necessary that the T_g of powder should be sufficiently low to ensure

a lower viscosity in its molten state. In order to solve this contradiction, crystallizable moieties are under consideration for introduction into resins.

Dendritic polymers have attracted increasing interest from the polymer science community during the past 15 years. These materials present a new, and well-defined architecture, and a large degree of functionality in a molecule. A wide variety of dendritic polymers with different chemical structures have been synthesized.^{3–5} However, commercial applications of these materials have not been widely realized until recently. Many potential applications under investigation, such as coatings and rheology modifiers, make use of the important architectural characters of dendritic polymers. Their larger number of end-groups, compact molecular shape, and fewer chain entanglements provide low melting viscosity, better miscibility, and higher reactivity. Hult et al.^{5–7} have successfully investigated the applications of dendritic polymers in UV curing coating.

Dendritic polymers are usually unable to crystallize due to their highly branched topology.⁸ However, crystallization can be induced by the attachment of long alkyl chains to dendritic polymers.^{9–11} Hult et al.¹² described the synthesis of semi-crystalline resins based on hyperbranched polyesters by grafting crystalline segments at first and then end-capping with UV-curable methacrylic groups. These semi-crystalline resins are promising for use as low-temperature UV-curable powder coatings.

This article describes the synthesis of semi-crystalline resins by modifying hydroxyl groups of dendritic poly(ether-amide) (DPEA-OH). The thermal behavior

Correspondence to: W. Shi (wfshi@ustc.edu.cn).

Supported by a grant from the National Natural Science Foundation of China (No. 50233030).

and crystalline properties, as well as photopolymerization kinetics, and the final residual unsaturation were investigated.

EXPERIMENTAL

Materials

DPEA-OH was synthesized in our laboratory starting from pentaerythritol by a divergent procedure.¹³ Toluene-2,4-diisocyanate (TDI) and β -hydroxyethyl acrylate (HEA) were supplied from the First Reagent Co. of Shanghai, China. Octadecyl isocyanate was supplied from Aldrich Chemical Co., Germany. Benzoyl-1-hydroxyl-cyclohexanol (Irgacure 184) as a photoinitiator was supplied from Ciba-Geigy, Switzerland. Other chemicals were purchased from Shanghai Chemical Co. of China. All chemicals were used as received.

Synthesis

The semi-crystalline dendritic resins were synthesized via a three-step procedure. Equal moles of TDI and HEA were dissolved in CH_2Cl_2 . The mixture was stirred under 40°C for 8 h, then a given amount of DPEA-OH in DMF was added and stirred under 50°C for 12 h. Finally, the calculated amount of octadecyl isocyanate, according to the residual hydroxyl groups of DPEA-OH, was added and stirred under 50°C for 12 h. The reaction mixture was precipitated into distilled water, then washed with acetone, and finally dried under a vacuum system giving a white powder. Two kinds of semi-crystalline resins with different substitution degrees of TDI-HEA and octadecyl isocyanate were synthesized, named DPEA-A and DPEA-B, respectively.

¹H-NMR (δ , CDCl_3): 0.88 (CH_3), 1.14–1.62 ($\text{CH}_3(\text{CH}_2)_{16}$), 1.82 (CH_3 next to benzene ring), 2.22 ($\text{OCH}_2\text{CH}_2\text{CONH}$), 2.6–3.6 ($\text{CONHCH}_2(\text{CH}_2)_{16}\text{CH}_3$ and $\text{C}^4\text{CH}_2\text{OCH}_2$), 4.34–4.44 ($\text{C}^4\text{CH}_2\text{O}$ and CH_2OCONH next to benzene ring), 5.88–6.45 ($\text{CH}_2=\text{CH}$ -), 7.09, 7.5, 8.04 (CH of benzene ring) ppm.

FTIR (KBr): 3300 cm^{-1} (N-H, stretching), 1660 cm^{-1} (C=O), 1560 cm^{-1} (N-H bending).

Measurements

The infrared (FTIR) spectra were recorded with a MAGNA-IR 750 spectro meter (Nicolet Instrument Co., Wisconsin). The nuclear magnetic resonance (NMR) spectra were recorded with a DMX-500 (Bruker Co., Zurich, Switzerland) using CDCl_3 as a solvent. X-ray diffraction (XRD) measurements were carried out at room temperature using a D/MAX-YA rotating anode X-ray diffractometer (Rigaku Co., Tokyo, Japan) with a CuK_α irradiation and graphite

monochromator. The diffraction patterns were determined over a range of diffraction angle $2\theta=10\text{--}40^\circ$. Differential scanning calorimetry (DSC) was performed on a Perkin Elmer Pyris 1 DSC (Norwalk, CT), calibrated according to standard procedures, using a heating rate of $10^\circ\text{C min}^{-1}$.

The photopolymerization rates (R_p) were monitored by a modified CDR-1 DSC (Shanghai Balance Instrument Co., Shanghai, China). The photoinitiator, Irgacure 184, was applied in the concentration of 4 wt %. The samples melted at 140°C in N_2 , then a UV spot-cure system BHG-250 (Mejiro Precision Co., Tokyo, Japan) was used for irradiating the samples. The incident light intensity at the sample was measured to be 2.04 mW cm^{-2} . The digitized data was analyzed by the software Origin 5.0 on a personal computer. The unsaturation conversion (P) was calculated by the following formula: $P = H_t/H_\infty$, where H_t is the heat effect within t seconds, H_∞ is the heat effect of 100% conversion of double bonds. The DSC curve was adjusted by the weight of a sample (g). The R_p was defined by $\text{mmol}_{\text{C}=\text{C}}\text{ g}^{-1}\text{ s}^{-1}$, namely, the variation of double bond concentration (mmol g^{-1}) per second.¹⁴ For calculating the R_p and H_∞ , the value for the heat of polymerization $\Delta H_0=86\text{ J mmol}^{-1}$ (per acrylic double bond) was taken.¹⁵ The concentration of double bond was calculated from the ¹H-NMR measurements.

Thermogravimetric analysis (TGA) was made on a Shimadzu TA-50 (Rigaku Co.) using a heating rate of $10^\circ\text{C min}^{-1}$ from 20 to 800°C . The thermal degradation temperature of the cured sample was taken as the temperature at which 5% weight loss. The pendulum hardness and pencil hardness of the cured films were determined using a QBY apparatus and a QHQ-A apparatus (Tianjin Instrument Co., Tianjin, China), respectively.

UV curing

The DPEA-A and DPEA-B samples were mixed with Irgacure 184 (4 wt %), flow-out at 140°C and applied on glass plates with a $100\text{ }\mu\text{m}$ applicator, respectively. These sample plates were then exposed to a UV lamp (1 kW, 80 w cm^{-1} , made by Lantian Co., Beijing, China) at variable conveyor speeds in air.

RESULTS AND DISCUSSION

Synthesis

The synthesis of DPEA-A and DPEA-B, and their idealized molecular structures are schematically outlined in Figure 1. The reaction of hydroxyl group of HEA with isocyanate group of TDI mostly occurs at the para position of the methyl group in TDI. The small amount of side product, resulting from di-addition to TDI, can be removed by acetone at the last treatment

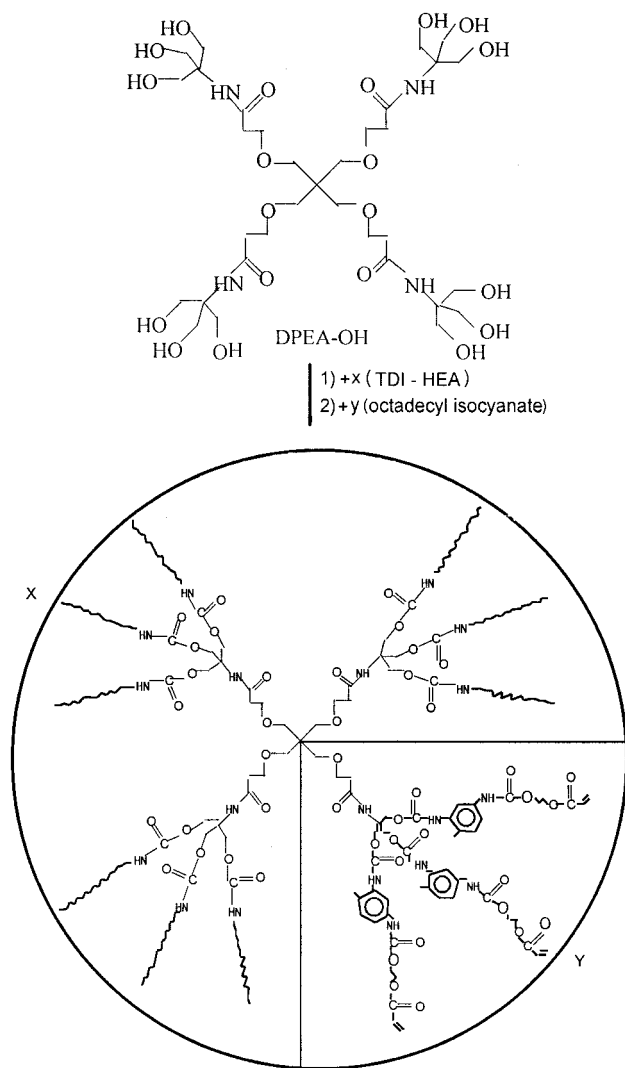


Figure 1 Schematic outline of DPEA-A and DPEA-B synthesis.

step. The consumption of hydroxyl groups of HEA was confirmed by the disappearance of the IR absorption at 3380 cm^{-1} . The completion of the reaction between DPEA-OH with TDI-HEA and octadecyl isocyanate was confirmed by the disappearance of the IR absorption at 2250 cm^{-1} for isocyanate group.

The substitution degrees of TDI-HEA and octadecyl isocyanate were calculated from the $^1\text{H-NMR}$ spectra, using the signal intensities of the DPEA-OH scaffold and the two substituents. The $^1\text{H-NMR}$ spectrum of DPEA-A as an example is shown in Figure 2. The methylene proton next to amide bond shows 2 signals at 2.22 ppm for DPEA-OH. The methyl proton at long carbon chain ends can be assigned at 0.88 ppm for octadecyl isocyanate. The proton of the acrylic double bond exhibits three signals between 5.88 and 6.45 ppm. Using the intensity of three signals, 17 and 83% were obtained as the average substitution degree of TDI-HEA and octadecyl isocyanate, respectively. The

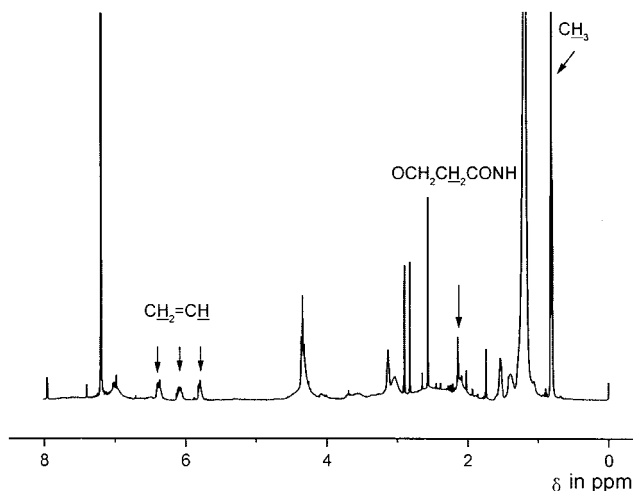


Figure 2 $^1\text{H-NMR}$ spectrum of SPEA-A.

calculated results with molar mass and double bond concentration from $^1\text{H-NMR}$ measurements are listed in Table I.

Semi-crystalline properties

Linear polymers are generally amorphous, crystalline, or liquid crystalline. Dendritic polymers exist generally in the amorphous state because of their highly branched architectures which make the molecules very hard to stack compactly. However, the nature of its end-groups has a great effect on the properties of a dendritic polymer.¹⁶ By changing the end-groups, e.g., grafting long alkyl chains, the morphology of a dendritic polymer can be changed from amorphous to semi-crystalline. The XRD patterns for DPEA-OH, DPEA-A, and DPEA-B are shown in Figure 3. It can be found that DPEA-OH is amorphous, while strong peaks at 22.7° , and also side peaks at 19.3 , 19.6 , and 21.3° are observed from the XRD patterns of both DPEA-A and DPEA-B. This indicates that crystallization was introduced into both DPEA-A and DPEA-B.

TABLE I
Characterization Data on DPEA-A and DPEA-B

Samples	Content of modifier (%)		$\bar{M}_{n(\text{NMR})}^a$	C_D (mmol/g) ^b
	TDI-HEA (x%)	Octadecyl isocyanate (y%)		
DPEA-A	17	83	4060	0.46
DPEA-B	43	57	3990	1.18

^a Calculated from $^1\text{H-NMR}$ measurements according to the following formula:

$$(\bar{M}_n) = \frac{8[L(\text{CH}=\text{CH}_2) \times 290 + L(\text{CH}_3) \times 295]}{31(\text{OCH}_2\text{CH}_2\text{CONH})} + 790$$

^b Calculated from $^1\text{H NMR}$ measurements.

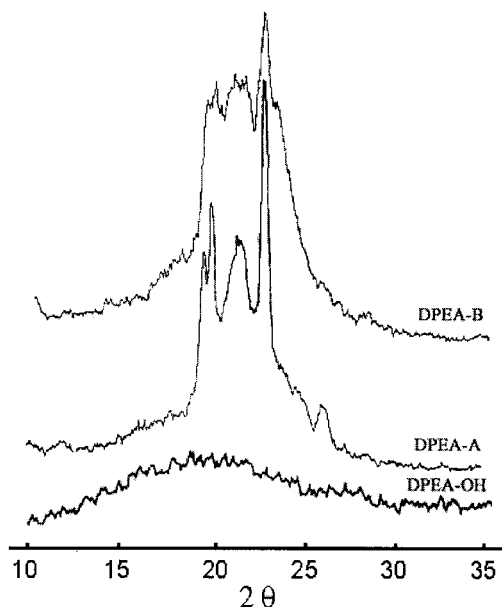


Figure 3 XRD spectra of DPEA-OH, DPEA-A, and DPEA-B.

Moreover, it can be seen that DPEA-A has a higher degree of crystallinity as shown by its stronger XRD peaks. This can be explained by the higher density of long alkyl chains emitting from the branched interior, which makes themselves orient or align in regular arrays easily. From the DSC measurements shown in Figure 4, both DPEA-A and DPEA-B exhibit several peaks with a main peak at 120°C. This can be interpreted as due to the formation of several crystallites with different molecular structures resulted from side-reactions with TDI and incomplete reactions. The data from DSC measurements are presented in Table II. It can be found that the melting enthalpy (ΔH) of 114 J/g

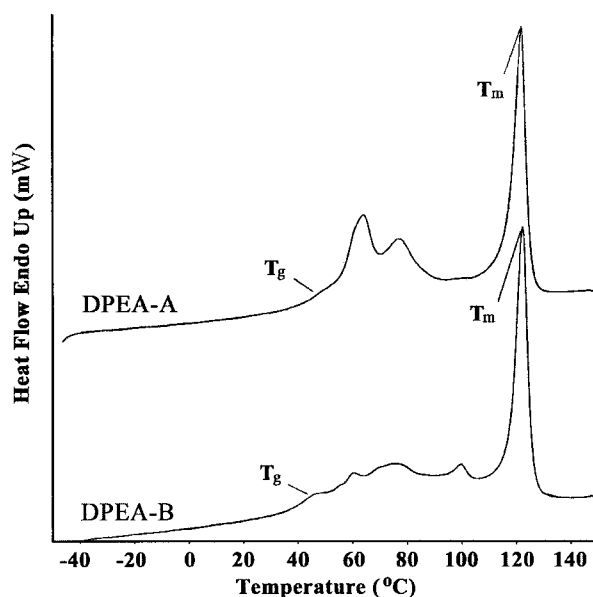


Figure 4 DSC spectra of DPEA-A and DPEA-B.

TABLE II
Thermal Behavior of Semi-Crystalline
DPEA-A and DPEA-B

Samples	T_g (°C)	T_m (°C)	ΔH (J/g)	T_d (°C)
DPEA-A	45	122	114	200
DPEA-B	41	123	86	208

for DPEA-A is higher than that of 86 J/g for DPEA-B, which is the same trend as the result from XRD measurement.

Thermal behavior

The thermal behaviors of DPEA-A and DPEA-B are listed in Table II. It can be seen that their T_g are 45 and 41°C, respectively, compared with -20°C for DPEA-OH.¹³ As is well known, the inter-molecular crystallization and intra-molecular crystallization are obtained when an amorphous dendritic polymer is grafted with longer alkyl chains, causing an increase of T_g . The T_g of DPEA-A is higher than that of DPEA-B because the former contains more longer alkyl chains, which result in a higher degree of crystallinity than the latter. Both DPEA-A and DPEA-B materials may be used as pre-polymers of UV-curable powder coatings, because of their suitable T_g (above 40°C), to ensure the stability of powder during handling, transportation, and storage.¹⁷ From Table II, T_m of DPEA-A and DPEA-B are 122 and 123°C, respectively. This indicates that two semi-crystalline materials can be molten and flow-out at around 140°C, which makes them suitable for coating on several types of heat sensitive substrates.¹⁸

Photopolymerization rate

Both DPEA-A and DPEA-B containing acrylic end-groups, can be cured by efficient UV irradiation via a radical polymerization mechanism. The final properties of a powder coating depend strongly on its photopolymerization kinetics.¹⁷ The most important pa-

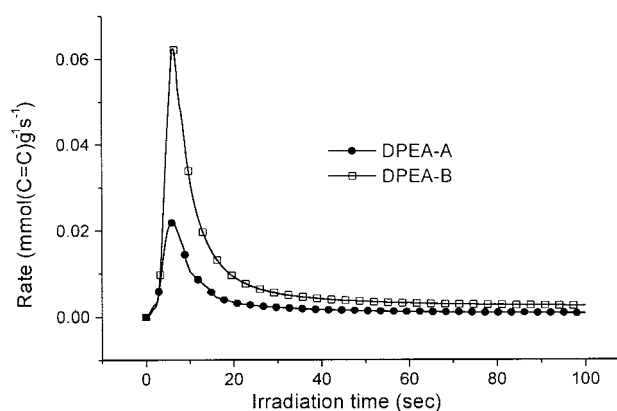


Figure 5 Photopolymerization rates of DPEA-A and DPEA-B.

rameters characterizing the photopolymerization kinetics are the rate at peak maximum (R_p^{\max}) and the final conversion of unsaturation (P^f). The photopolymerization rates and the unsaturation conversion of DPEA-A and DPEA-B are shown in Figure 5 and Figure 6, respectively. It can be found that the R_p^{\max} of DPEA-A and DPEA-B are $0.0218 \text{ mmol}_{\text{C}=\text{C}} \text{ g}^{-1} \text{ s}^{-1}$ and $0.0626 \text{ mmol}_{\text{C}=\text{C}} \text{ g}^{-1} \text{ s}^{-1}$, respectively. The much higher R_p^{\max} of the latter attributes to its higher concentration of double bonds. DPEA-A and DPEA-B have almost the same P^f of around 64%.

FTIR spectra of the cured DPEA-A and DPEA-B films under 1 kW UV lamp irradiation in air reveal about 5 and 20% of residual unsaturation, respectively, which are lower than those cured under a spot-cure in Photo-DSC. This is because the higher P^f of double bonds can be obtained with higher incident light intensity. The higher residual unsaturation in the UV-cured DPEA-B film is attributed to its dense crosslink network, which prohibits some double bonds from taking part in further polymerization.

Properties of the UV-cured films

The thermal degradation temperature of the UV-cured films of DPEA-A and DPEA-B from TGA measurements are 200 and 208°C, respectively, as shown in Figure 7. It can be also found that the rate of weight loss for DPEA-B film is lower than that for DPEA-A film, which is attributed to the former's higher crosslink density. The pendulum hardness of the UV-cured DPEA-A and DPEA-B films are 310 and 340 s, respectively; corresponding pencil hardness are B and 2H. This further indicates that the UV-cured DPEA-B film has higher crosslink density.

CONCLUSIONS

To explore the possibility using dendritic polymers as UV-curable prepolymers in powder coating systems, two kinds of semi-crystalline resins were synthesized

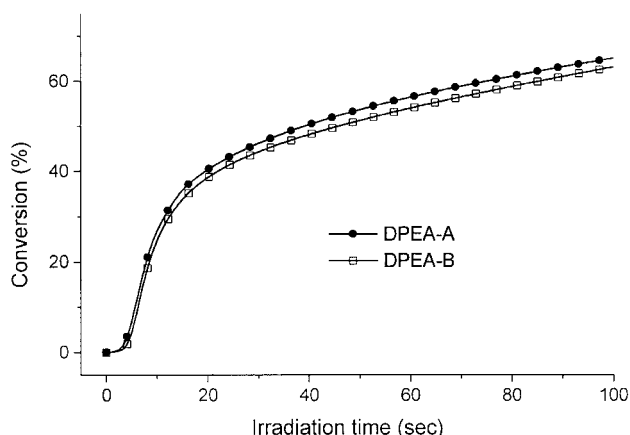


Figure 6 Unsaturation conversion of DPEA-A and DPEA-B.

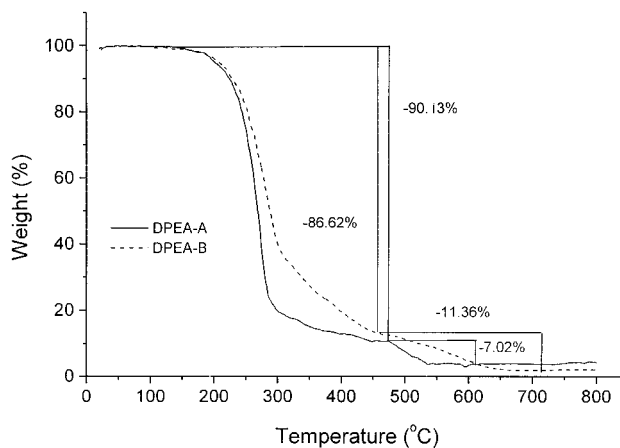


Figure 7 TGA thermograms of the UV-cured DPEA-A and DPEA-B films.

by grafting DPEA-OH with different ratios of octadecyl isocyanate to TDI-HEA. The density of octadecyl isocyanate chains grafted to DPEA-OH has a positive effect on crystallinity. These semi-crystalline resins have a T_g of above 40°C and a T_m of around 120°C. They were UV-cured in the presence of a photoinitiator to yield films with high unsaturation conversion after melting. The synthesized semi-crystalline poly(etheramide)s are very promising for use as UV-curable powder coating resins.

References

- Saskia, U. L.; Richard, A. B.; Nico, W. F. RadTech Europe'99 Conference Proceedings, 1999, 607.
- Skinner, D. RadTech Europe'99 Conference Proceedings, 1999, 599.
- Voit, B. J Polym Sci Part A Polym Chem 2000, 38, 2505.
- Chow, H. F.; Mong, T. K. K.; Nongrum, M. F.; Wan, C. W. Tetrahedron 1998, 54, 8543.
- Hult, A.; Johansson, M.; Malmström, E. Adv Polym Sci 1999, 1, 1.
- Johansson, M.; Glauser, T.; Rospo, G.; Hult, A. J Appl Polym Sci 2000, 75, 612.
- Wei, H. Y.; Lu, Y.; Shi, W. F.; Yuan, H. Y.; Chen, Y. L. J Appl Polym Sci 2001, 80, 51.
- Kim, Y. H. J Polym Sci Part A Polym Chem 1998, 6, 1685.
- Schenning, A. P. H. J.; Elissen-Román, C.; Weener, J. W.; Baars, M. W. P. L.; van der Gaast, S. J.; Meijer, E. W. J Am Chem Soc 1998, 120, 8199.
- Malmström, E.; Jonasson, M.; Hult, A. Macromol Chem Phys 1996, 197, 3199.
- Sunder, A.; Bauer, T.; Mülhaupt, R.; Frey, H. Macromolecules, 2000, 33, 1331.
- Hult, A.; Johansson, M.; Jansson, A.; Malmström, E. RadTech Europe'99 Conference Proceedings, 1999, 634.
- Wei, H. Y.; Shi, W. F. Chem J Chin Univ 2001, 22, 1605.
- Fouassier, J. P.; Rabek, J. F. Radiation Curing in Polymer Science and Technology; Elsevier: New York, 1993, Vol. 1, p 392.
- Andrzejewska, E.; Andrzejewski, M. J Polym Sci Part A Polym Chem 1998, 36, 665.
- Percec, V.; Chu, P.; Ungar, G.; Zhou, J. J Am Chem Soc 1995, 117, 11441.
- Maetens, D. RadTech North America'98 Conference Proceedings, 1998, 170.
- Buyssens, K. RadTech Europe'99 Conference Proceedings, 1999, 622.